INSTITUTE OF PHYSICS PUBLISHING NETWORK: COMPUTATION IN NEURAL SYSTEMS

Network: Comput. Neural Syst. **14** (2003) 17–33 PII: S0954-898X(03)56977-9

Coincidence detection with dynamic synapses

Lovorka Pantic, Joaquín J Torres[1] and Hilbert J Kappen

Department of Medical Physics and Biophysics, University of Nijmegen,
Geert Grooteplein Noord 21, 6525 EZ Nijmegen, The Netherlands

Received 2 February 2002, in final form 26 November 2002
Published 17 January 2003
Online at stacks.iop.org/Network/14/17

Abstract

Recent experimental findings show that the efficacy of transmission in cortical synapses depends on presynaptic activity. In most neural models, however, the synapses are regarded as static entities where this dependence is not included. We study the role of activity-dependent (dynamic) synapses in neuronal responses to temporal patterns of afferent activity. Our results demonstrate that, for suitably chosen threshold values, dynamic synapses are capable of coincidence detection (CD) over a much larger range of frequencies than static synapses. The phenomenon appears to be valid for an integrate-and-fire as well as a Hodgkin–Huxley neuron and various types of CD tasks.

1. Introduction

Recent experimental studies of cortical cells show that the postsynaptic potential is a dynamical quantity which depends on the presynaptic activity [1, 2, 5–8]. After transmission of an action potential (AP) the synapse needs to recover before it restores to its original strength. Thus, the amplitude of the postsynaptic response tends to decrease with increasing input frequency of presynaptic spike trains. The behaviour is known as short-term depression and phenomenologically is well explained by the *dynamic* model of synapses introduced in [1]. In contrast, the standard (static) model of synapses does not display such a complex synaptic behaviour. The postsynaptic responses have constant strength which is insensitive to the input frequency. The fact that synaptic strength is a function of neural activity greatly affects our traditional view of neural processing such as recurrent excitation, cell assemblies and memory as attractors.

To explore the possible role of the activity-dependent synapses in neuronal transmission properties, we analyse the responses of a postsynaptic neuron to temporal structures of the afferent activity. Motivation for this analysis arises from the observation that in a variety of sensory systems, there is physiological evidence indicating that precise temporal correlations among groups of neurons appear to encode different stimulus features [9–11] or may be

[1] Present address: Department of Electromagnetism and Material Physics, University of Granada, E-18071 Granada, Spain.

0954-898X/03/010017+17$30.00

an important factor for some mechanisms of selective attention [12]. In addition, it is also established that synchronous increase in the firing rates or correlated bursting activity might be relevant signal carriers in some behavioural situations [9]. Thus, detection of the synchronized firing patterns such as coincident spike trains, synchronous rate changes or correlated bursts seems to be an important neuronal mechanism and as suggested in [3, 4, 16] a physiologically plausible operation mode of cortical neurons.

The capability of the neuron with static synapses to perform a coincidence detection (CD) has been thoroughly studied in [17, 19, 21]. In [17] it is shown that the CD properties are influenced by the parameters of the neuron model and by the number of synapses and their mean activity. In particular, these authors show that there is a threshold value that maximizes the CD abilities and they discuss potential adaptive mechanisms that can control the threshold.

In [1, 2] it is shown that the detection of the rate changes is enhanced with synaptic depression. In [20], it is shown that dynamic synapses are capable of detecting correlations between afferent neurons, even when the total mean firing rate is unchanged. Static synapses fail on this task. However, in both these studies the comparison was made for certain fixed parameter choices, such as overall synaptic strength, neural threshold value, input spike frequency and synaptic recovery time. The aim of our study is to investigate the CD properties for static and dynamic synapses, when these parameters are varied. Our definition of CD contains both the coincident firing of subgroups of presynaptic cells, as studied in [3, 4, 16], synchronous bursts [20], as well as the synchronous increase of firing rate [1, 2].

In section 3.1 we present numerical and analytical results that show the detection abilities of an integrate-and-fire (IF) neuron with parameters typical for cortical cells. We explore regions in the space of parameter values where it is possible to find robust CD when a subset of the afferent inputs is assumed to receive coincident spike trains. We conclude that with synaptic depression there exists a range of the threshold values which enable the CD over the large range of input frequencies. If the synaptic depression is not considered, the frequency window for detection is smaller and does not depend on the threshold value. We show analytically that the synaptic dynamics time constant (τ_{rec}) is a parameter which strongly affects the region of good detection in the frequency-threshold domain.

In section 3.2 we show that the conclusion about the enhanced CD with dynamic synapses also holds for the more complex Hodgkin–Huxley (HH) neuron model.

In section 3.3 we show that this effect is robust even when the coincident events are distorted by temporal jitter.

In section 3.4 we consider the CD of synchronous rate changes. We demonstrate that detection of the rate changes also appears to be sensitive to the threshold value in the case of synaptic depression such that only optimally chosen threshold ensures detection. With static synapses it seems that tuning of the threshold values that enables this kind of detection is not possible. Finally we have included an appendix with derivations of our analytical results.

2. Models

We consider a single neuron that receives inputs from $N excitatory$ synapses. All inputs are modelled as Poisson processes with the same mean firing rate f. According to the model introduced in [1], the dynamics of each depressing synapse i is governed by the following three-state kinetic scheme:

$$\mathrm{d}x_i/\mathrm{d}t = z_i/\tau_{rec} - U_{SE}x_i\delta(t - t_{sp}), \tag{2.1}$$

$$\mathrm{d}y_i/\mathrm{d}t = -y_i/\tau_{in} + U_{SE}x_i\delta(t - t_{sp}), \tag{2.2}$$

$$\mathrm{d}z_i/\mathrm{d}t = y_i/\tau_{in} - z_i/\tau_{rec}, \tag{2.3}$$

where x_i, y_i, z_i are, respectively, the fractions of neurotransmitters in the recovered, active and inactive states. $\tau_{in} = 3$ ms and $\tau_{rec} = 800$ ms are, respectively, the time constants for inactivation and recovery processes. $U_{SE} = 0.5$ represents a fraction of the recovered neurotransmitter released by each presynaptic event. The postsynaptic somatic current from synapse i is proportional to the fraction of neurotransmitter in the active state, that is, $I^i_{syn}(t) = A_{SE} \cdot y_i(t)$, where the parameter A_{SE} is the maximal postsynaptic current emitted when the total amount of neurotransmitter is in the active state[2]. A natural and simple way to define the *static* (non-depressing) synapse from this model is to consider[3] $x(t) = 1\,\forall t$. Thus, the system (2.1)–(2.3) reduces to equation (2.2). Under this assumption it can be shown that the amplitude of the individual postsynaptic current does not depend on the frequency of the input train. For both descriptions, dynamic or static, the total synaptic current is given by $I_{syn} = \sum_{i=1}^{N} I^i_{syn}$.

We use a standard IF neuron, whose membrane potential satisfies

$$\tau_m \, \mathrm{d}V/\mathrm{d}t = -V + R_{in} I_{syn}. \tag{2.4}$$

Parameters have been typical for cortical cells [1, 15], i.e. an input resistance $R_{in} = 100\ \mathrm{M}\Omega$ and membrane time constant $\tau_m = 15$ ms. We have considered the threshold for firing $V_{th} = 13$ mV above the resting potential $V_{rest} = 0$. Every time that EPSP reaches V_{th}, an AP is generated and the membrane potential is reset to zero. We choose an absolute refractory period $\tau_{ref} = 5$ ms.

3. Results

3.1. Detection of coincident spike trains

We analyse the responses of a neuron that receives input from $N = 1000$ afferents where a subset of $M = 200$ is stimulated by identical (Poisson) spike trains. We consider that M correlated inputs constitute a 'signal' term while the remaining $N - M$ synapses, stimulated by uncorrelated spike trains, represent a 'noise' term in the synaptic input[4]. This (simplified) concept of signal may not correspond to a biologically plausible situation but enables a derivation of an analytical result that relates relevant model parameters. We will show, however, that conclusions will also be valid for other more realistic CD tasks.

In figure 1 we illustrate CD capabilities for the IF neuron with dynamic and static synapses. For the dynamic synapse, the parameter A_{SE} has been set to $A_{SE} = 42.5$ pA to enable CD at a frequency of 10 Hz (for the chosen threshold value of $V_{th} = 13$ mV). For a static synapse we have adjusted $A_{SE} = 8.5$ pA to obtain the same output rate at 10 Hz for both synaptic descriptions.

Figure 1 shows that the neuron with dynamic synapses is capable of CD at 5, 10 and 30 Hz, whereas the neuron with static synapses only at 5 and 10 Hz. These results depend on the parameters of the model, most importantly, on the threshold value (V_{th}) and the input frequency (f). To find the parameter regions of good detection we have varied the frequency and threshold. For each (f, V_{th}) the following quantities have been computed:

[2] Note that synaptic conductance rather than the synaptic current depends directly on $A_{SE} \cdot y_i(t)$ but this quantity will approximate the current when the membrane potential is below threshold.

[3] An equivalent definition is to consider $\tau_{rec} \to 0$.

[4] For integration of the differential equations (2.1)–(2.4) we have used the Runge–Kutta fourth-order method with a small time step of 0.05 ms.

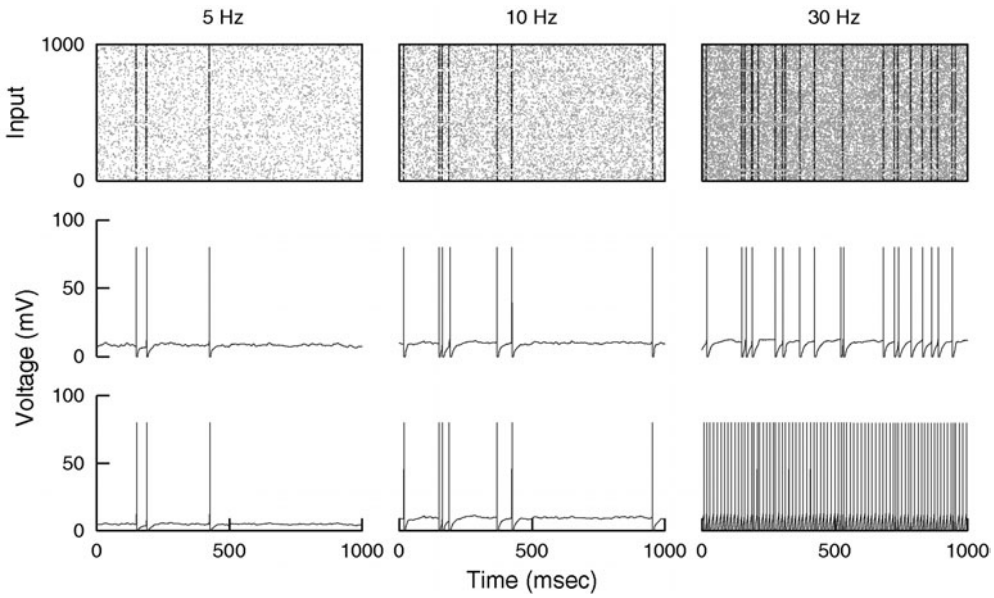

Figure 1. Spike detection in a system consisting of a single IF neuron with parameters typical for cortical pyramidal cells. The neuron receives $N = 1000$ synaptic inputs where 20% are randomly correlated (dark grey dots) at three input frequencies of 5, 10 and 30 Hz. The panels represent from top to bottom, the input pattern, membrane potential for the neuron with excitatory dynamic synapses and excitatory static synapses, respectively.

(a) the number of coincident-input-events[5] N_{inputs},
(b) the number of output spikes occurring immediately (within the time-window of $\Delta = 5$ ms which corresponds approximately to the EPSP rise time) after the coincident-input-events, that is, *hits*(N_{hits}),
(c) the number of output spikes that are not *hits*, that is, *false-hits* (N_{falses}),
(d) the number of coincident-input-events that did not result in output spikes within the time-window Δ, that is, *failures* for firing ($N_{failures}$).

We have defined the CD error as

$$\text{Error} = \frac{N_{falses} + N_{failures}}{N_{inputs}}. \tag{3.1}$$

Note that the CD error can be (much) larger than 1 when a low threshold produces a large number of 'false-hits'. Figure 2(A) (top) shows the CD error as a function of frequency and threshold, computed numerically for the neuron with either dynamic or static synapses. The black area is the area of 'false-hits' where the EPSP due to the noise is high enough to cause repetitive firing. The grey area (area of 'failures') represents the region where detection is poor due to the fact that the total EPSC of the signal and noise is not sufficient to push the EPSP across the threshold. The light area shows the region where CD occurs with a low percentage of errors. The main conclusion that arises is that for some optimal threshold value the frequency window for CD is wider in the dynamic than in the static case. For a static synapse, no matter how low or high the threshold value is, the frequency window is no wider than about 10 Hz.

[5] The 'coincident-input-events' are the coincident afferent activity that occurs in a time interval of length T. On average $N_{inputs} = fT$, but an individual trial may deviate from this average (for an illustration, see figure 1 where $N_{inputs} = 3$ at 5 Hz).

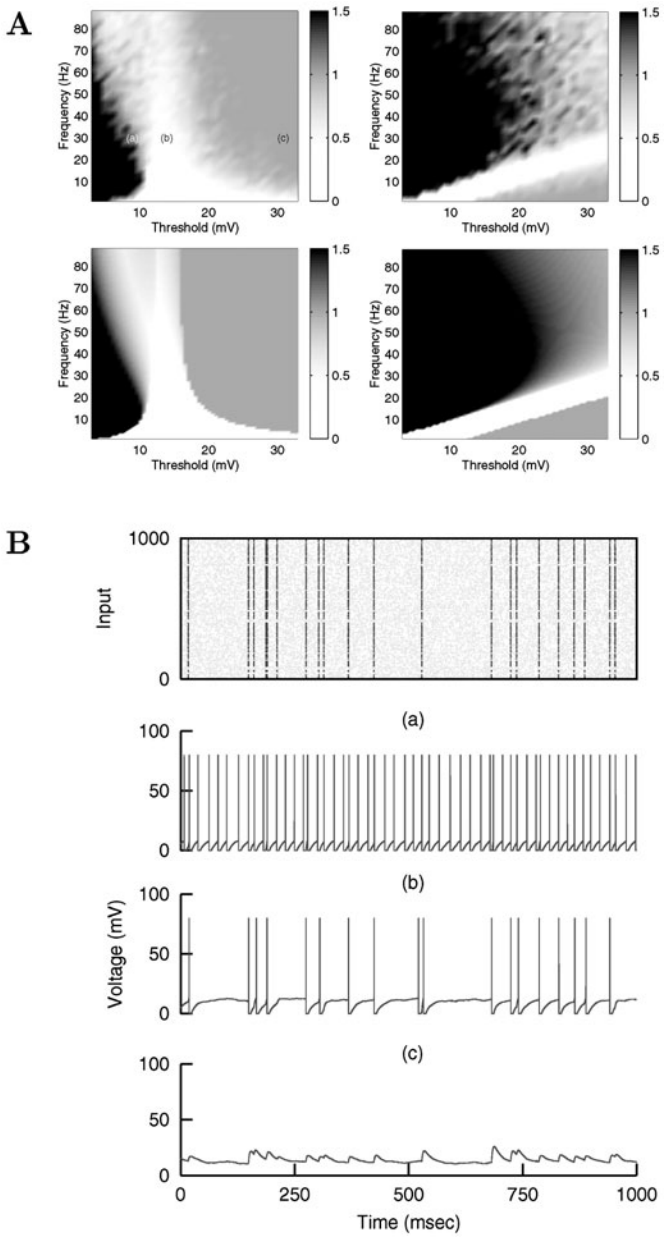

Figure 2. Detection abilities of the IF neuron. (A) (Top): the regions of detection found numerically for the IF neuron with either dynamic (left) or static (right) synapses, respectively, where 20% of the synapses receive correlated spike trains. The light area lying inside the contour is a region for which the neuron is able to detect the signal with a low percentage of errors. The black and grey regions are the zones with a high percentage of errors. Colour coding is identical in all subfigures. To obtain a numerical estimate for the CD error (see equation (3.1)), we use a simulation time window that has been adapted to input frequency, i.e. $T = \frac{100}{f}$. (Bottom) Figures represent the analytical result (see appendix). (B): (a)–(c) show the typical behaviour occurring in the areas marked with (a)–(c) in panel (A). From top to bottom, they represent the synaptic input at 30 Hz, membrane potential for the threshold values of 8 mV (false-hits), 13 mV (hits), 30 mV (failures), respectively.

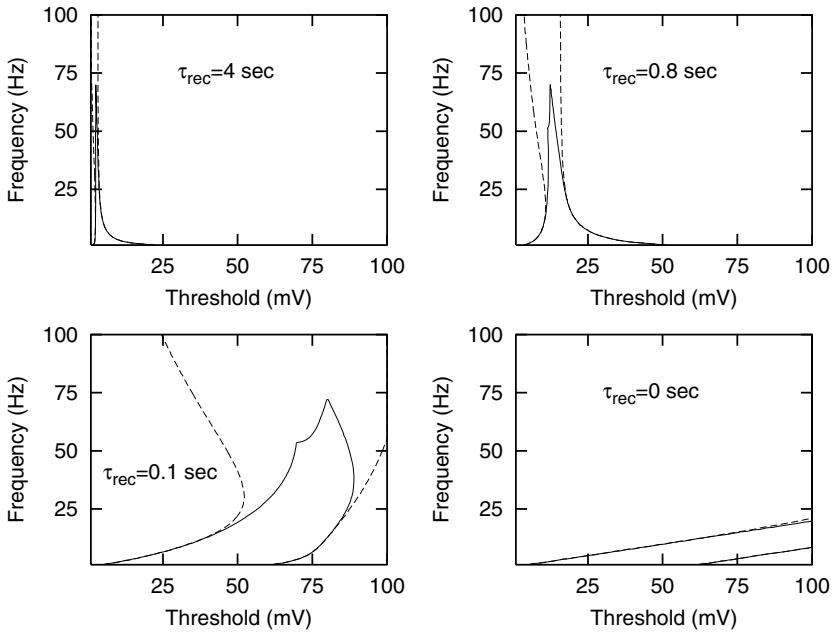

Figure 3. Regions of detection computed analytically for four different values of τ_{rec} and the same values of other parameters (note that $A_{SE} = 42.5$ pA in all figures). The value of $\tau_{rec} = 0$ ms corresponds to the non-depressing (static) synapse. The dashed (solid) curve corresponds to an analytically found contour line when Error = 1 (Error = 0.4).

For a dynamic synapse, however, there is an optimal threshold that ensures good CD for any frequency between 0–50 Hz. Figures 2(B) illustrate the typical firing behaviour occurring for three different parameter choices.

For the IF neuron, it is possible to approximately compute the CD behaviour analytically. The total synaptic current is composed of both signal and noise contributions, where the signal contribution comes from the M coincident afferents, and the noise contribution comes from the $N - M$ independent afferents. The noise contribution consists of a mean plus fluctuations. The probability that the neuron that receives this stochastic input will fire is given by a first passage time problem [22], which in general, cannot be solved analytically. We use the Arrhenius approximation also discussed by [22] to compute this first passage time problem. We show good agreement between our analytical results and numerical simulations in figures A.1, A.2, except for low frequency when the first passage problem is not well approximated by the Arrhenius ansatz. However, we also show that when the number of afferent neurons N is large the fluctuations can be ignored altogether and the CD error can be well approximated using the mean synaptic noise current only (figure A.3). Subsequently, we compute the signal contribution to the current in this same approximation. Using these results we analytically compute the phase diagram in figure 2(A) (bottom).

The numerical as well as analytical results, indicate that there are apparent differences between areas of detection for dynamic and static synapses. To examine how CD depends on the degree of depression, we have varied the time constant for recovery τ_{rec}. Figure 3 illustrates that τ_{rec} strongly affects the boundaries of (good) detection. It can be noticed that for any $\tau_{rec} > 0$ there exists a threshold at which good detection occurs over a large range of frequencies. For increasing τ_{rec} this threshold moves to smaller values.

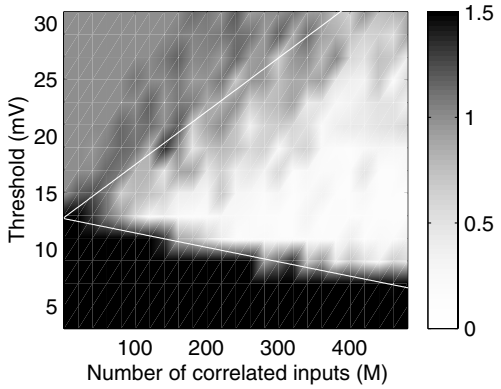

Figure 4. The range of the threshold values depends on the number of correlated inputs. The white line corresponds to the analytical contour line when Error = 1. Numerical data are given by different CD error values as shown by the colourbar. Numerical as well as analytical results are obtained at a frequency of 10 Hz. The numerical simulations lasted for $T = 10$ s.

The range of threshold values allowing detection is also affected by the number of afferents with coincident spike trains (M). Figure 4 shows numerical results indicating that the threshold range (at some fixed frequency) is an increasing function of the number M. The analytical results are in good agreement with numerical data and show a linear dependency on the number of coincident inputs.

The detection differences between the static and dynamic synapses as well as the specific 'bell-shaped' region of detection found for dynamic synapses can be explained intuitively in the following way. On timescales that are large in comparison to the membrane time constant, the membrane potential will attain a constant stationary value V. This value is equal to $V_{noise} = R_{in} I_{noise}$ in the absence of correlated inputs, with I_{noise} from equation (5.5) and equal to $V_{noise} + V_{signal}$, with V_{signal} given by equation (5.20) otherwise. Good detection requires that the threshold membrane potential must obey $V_{noise} < V_{th} < V_{noise} + V_{signal}$. For dynamic synapses, V_{noise} ($V_{noise} + V_{signal}$) is an increasing saturating (decreasing) function of input frequency (equations (5.5) and (5.20)). Therefore, the range of thresholds is largest for low frequencies. For increasing frequency the two curves (V_{noise} and $V_{noise} + V_{signal}$) approach each other giving the mentioned bell-shaped region. On the other hand, for static synapses, both potentials linearly depend on the input frequency leading to the 'band-shaped' region of detection presented in figure 2.

The bell-shaped detection behaviour of neurons with dynamic synapses, i.e. the fact that for some optimally chosen threshold value their CD property is good over a large range of frequencies, is also true for other types of CD tasks. In section 3.4 we will show this for the detection of synchronous increase of firing rates as considered by [1, 2]. In the discussion section, we provide an explanation why this is also true for the CD task defined by Senn *et al* [20].

3.2. Detection with the HH neuron

In this section we investigate whether our result regarding the enhanced detection ability with dynamic synapses is dependent on the neuron model. We have considered the HH neuron model with parameters as given in [13]. For this model, the value of the threshold is fixed and cannot be varied as in the IF model. Therefore we vary the strength of the synaptic current,

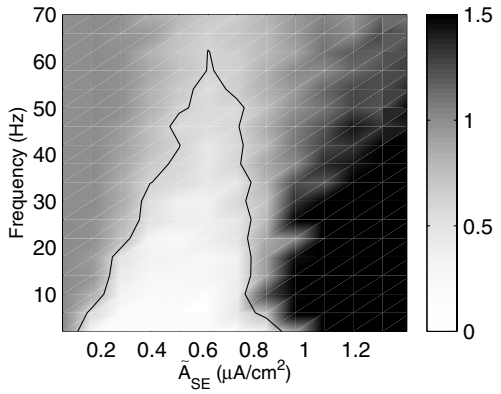

Figure 5. The detection ability of the HH neuron. We show the regions of detection found by the HH neuron with dynamic synapses where 10% of the synapses receive coincident spike trains. The light area inside the contour (solid black curve) denotes the region with Error < 0.6. The grey and black areas represent regions with a higher percentage of errors. To estimate the CD error, the numerical simulations lasted for $T = \frac{100}{f}$ s.

that is, the parameter[6] $\tilde{A}_{SE}$ instead of the threshold. The dynamic synapses are modelled as explained in section 2 with parameters $\tau_{rec} = 300$ ms, $\tau_{in} = 3$ ms and $U_{SE} = 0.5$. The frequency is varied in the range between 1 and 70 Hz, the percentage of coincident inputs considered here is 10% and the total number of afferents is $N = 1000$. For each value of frequency and $\tilde{A}_{SE}$, the CD error defined above has been computed as shown in figure 5. The black and grey regions represent the regions with a high number of 'false-hits' and 'failures', respectively, while the light region corresponds to the region of good detection. The figure shows that there is a range of synaptic-strength values that ensures good detection within the large frequency window. Thus, the dynamic synapses produce similar effects on the detection ability (i.e. the 'bell-shaped' region of detection) of both the HH neuron and the IF neuron.

3.3. Effect of jitter

Many experimental studies reveal that cortical neurons fire with high temporal precision but not exactly simultaneously as considered in the previous sections. Some studies report that timing differences of afferent firing are of the order of a few milliseconds [16]. To study the effect of temporal jitter on the coincident detection ability we assume that spikes arrive approximately at the same time but not exactly. We consider that $M = 200$ afferents fire at moments that are Gaussian distributed around a mean value with a standard deviation of $\sigma = 4$ ms [16] whereas the mean values are Poissonian distributed. The remaining $N - M$ synapses are independent Poisson spike trains as before. All afferents fire with the same input frequency f. For a sample of the data see figure 6. We analyse the detection ability of the neuron in the same manner as in the first part but the time window for detection (Δ) is from -3σ to 3σ centred on the mean signal time. The duration of the correlated activity is determined by the temporal jitter and to ensure no overlaps between two consecutive signal events, the input frequency f is varied within the range 1–30 Hz. To compute the CD error we use the same notions of *hits*, *false-hits* and *failures* as before, where we consider that if the neuron fires at least one time within the window Δ, such an event is defined as a 'hit'. If the neuron fails to fire within the window,

[6] $\tilde{A}_{SE}$ is the parameter A_{SE} (see section 2 and 3) in units of μA cm^{-2}.

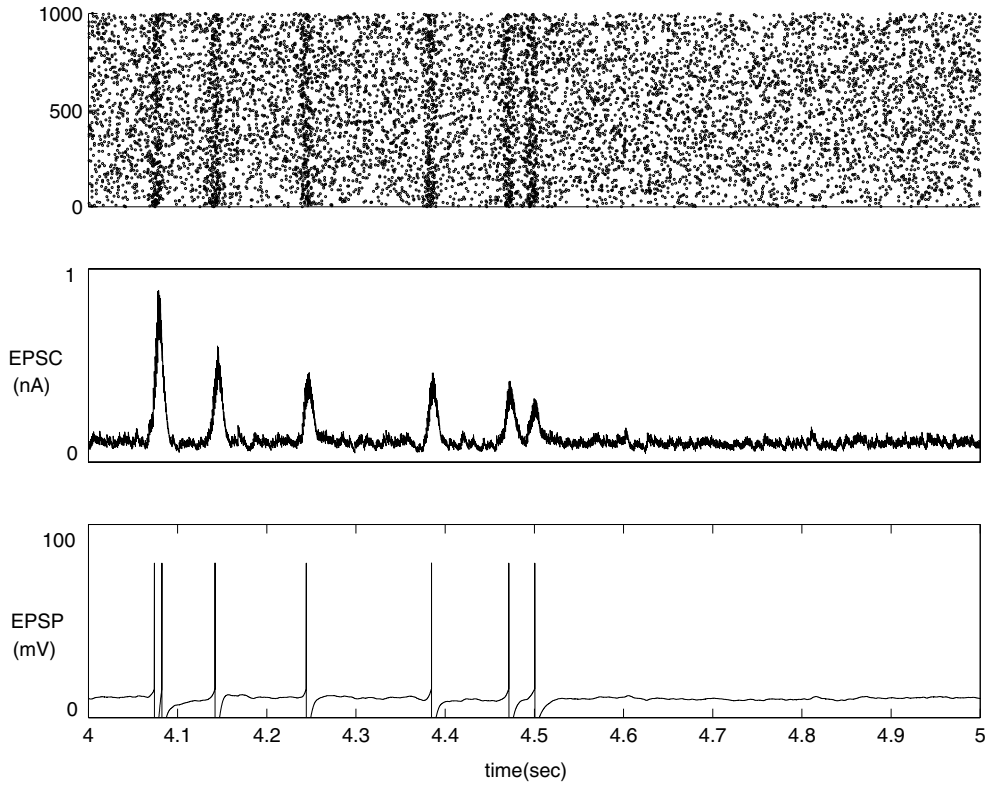

Figure 6. From top to bottom the figures show a raster plot of $N = 1000$ afferents where 20% are temporally correlated with a jitter of $\sigma = 4$ ms, total synaptic current and corresponding voltage response, respectively, at a frequency of 10 Hz.

the event is considered as a 'failure'. The 'hits' occurring in intervals between the windows are regarded as 'false-hits'. Figure 7 shows that qualitatively the same conclusions regarding the CD properties appear to be valid in this more realistic case. In short, for the dynamic case there exists an optimal range of threshold values which allows CD within a relatively large frequency window. The fact that similar detection properties are found with the temporal jitter is consistent with findings of Marsalek [19] showing that the IF neuron can perform CD as long as the jitter is smaller than the membrane time constant τ_m (15 ms in our case).

3.4. Detection of firing rate changes

The capability of a neuron to detect synchronous increases in the afferent firing rates has already been well explored in [1, 2]. In [1, 2] it was shown that for some selection of the relevant parameters, transient behaviour of the depressing synapses enables detection of the rate changes. Non-depressing synapses cannot give such transient responses. Here we study the dependence of this task on frequency and threshold. We assume a scenario when a population of $N = 1000$ afferents synchronously changes its firing rate every 500 ms. In figure 8 we show the membrane potential for various threshold values. Dynamic synapses can detect the moment of change in the firing rates if the threshold value is optimally chosen (third panel in the figure). In this case, detection is possible over a large range of frequencies (5–60 Hz). For somewhat

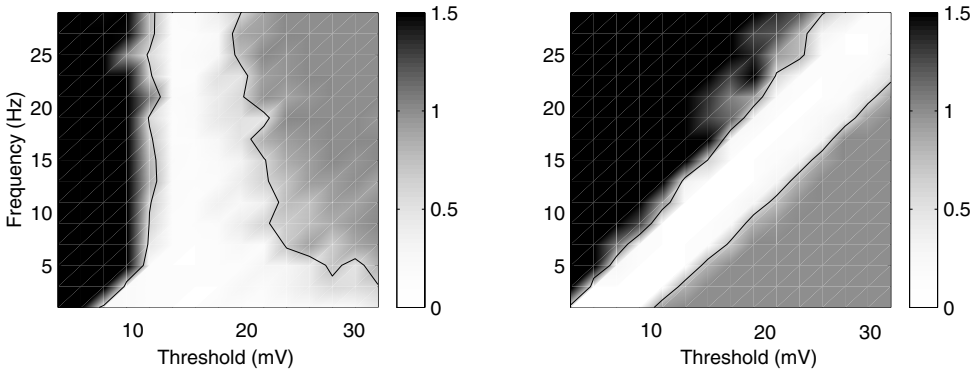

Figure 7. Left: regions of detection found numerically for an IF neuron with depressing (dynamic) synapses where 20% of afferents are temporally correlated with a jitter of $\sigma = 4$ ms. Right: the regions of detection for an IF neuron with non-depressing (static) synapses. Colour coding is given by the colour bar where white denotes low percentage errors (good detection) while grey and black mean high percentage errors (bad detection). The black curve denotes the contour line when Error = 0.5. The duration of the numerical simulation has been adapted to input frequency, $T = \frac{100}{f}$.

higher or lower threshold values, the neuron fails to fire or fires too often, respectively. Using equation (5.5) (in the appendix) we can easily estimate the area of good detection for this task. When the firing frequency of all afferent inputs changes from[7] f_1 to f_2, $(f_2 > f_1)$ the threshold must be chosen such that the response is transient, i.e. $Cf_2w(f_1) > V_{th} > Cf_2w(f_2)$ with $w(f)$ given by (5.5) and $C = R_{in}N\tau_{in}$ (see the appendix). For fixed $\delta f = f_2 - f_1$, $Cf_2w(f_1)$ is a decreasing function of f_1 for $\delta f \tau_{rec} U_{SE} > 1$, which is typically the case, and $Cf_2w(f_2)$ is an increasing function of f_2 and therefore of f_1. Both saturate to the same asymptotic value $CA_{SE}/\tau_{rec} \sim 16$ mV. Therefore for fixed δf, there is an optimal threshold value that allows good detection over a large range of frequencies. Since the two asymptotes converge to the same value, this range is limited to a maximum frequency, as a result of noise. The static synapse gives a response proportional to the average input frequency but there is no threshold value that ensures detection of the moments of abrupt rate changes.

4. Discussion

One of the important issues of neural functionality is the question whether the neuron is capable of extracting features of a particular signal from a noisy background. This issue is essential in biology, for instance when animals must distinguish regularities from a variety of changing and noisy input signals. Precise timing of APs may be used to convey such relevant information and CD as considered in this paper thus seems to be an important mechanism.

In this study we have shown how CD depends on the synaptic dynamics. Whereas static synapses require a frequency-dependent threshold value (or synaptic strength) for good detection, dynamic synapses can perform good CD over a large range of frequencies for one suitably chosen threshold value. This implies that no threshold adaptation mechanisms are required to perform well under variable conditions. In fact, the adaptation is done by the synapses themselves. We have shown that this general finding is true for various types of CD tasks, such as the detection of coincident spike trains or spike trains that are distorted with temporal jitter as well as the detection of synchronous rate changes.

[7] Note that $f_2 - f_1 > 0$ is necessary for the detection of rate changes.

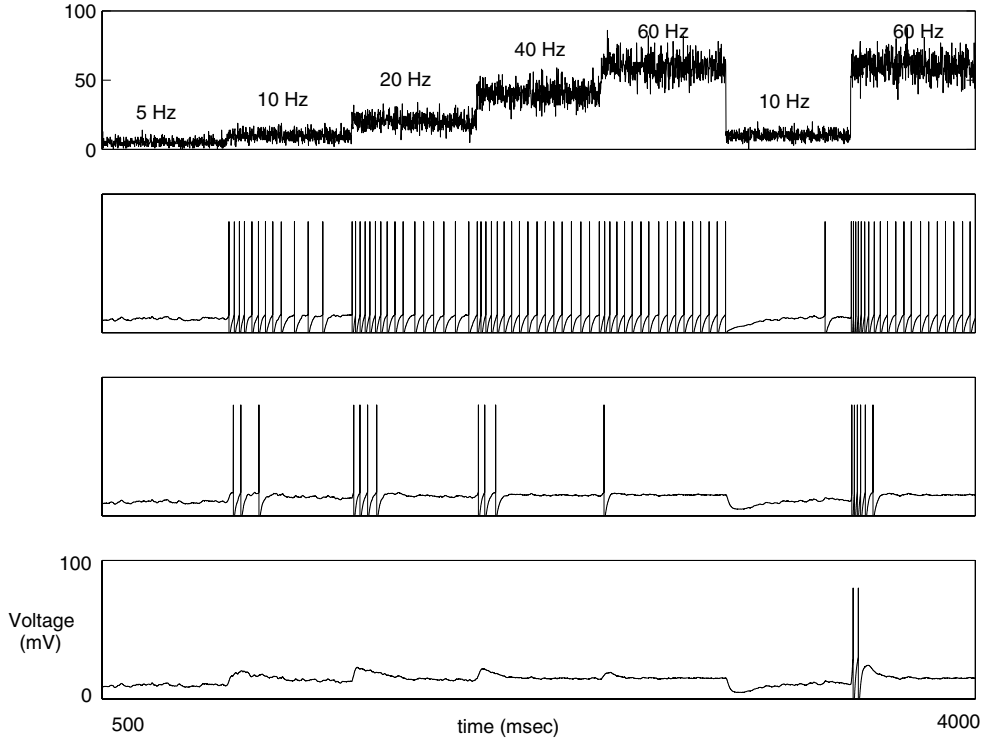

Figure 8. Detection of the changes in the firing rates. From top to bottom the panels represent the overall firing rate of the afferent population, corresponding voltage responses of the IF neuron with dynamic synapses at the threshold value of $V_{th} = 13, 17, 30$ mV, respectively.

The same finding is also valid for the detection of the correlated bursts [20]. In that study it was reported that neurons with dynamic synapses were capable of detecting correlations between afferent neurons during the stimulus, despite the fact that the mean firing rate (f) was unchanged. They assumed that every 50 ms another group of $M = 100$ neurons was bursting while the rest of the population fired at a reduced background frequency, such that the mean frequency over all $N = 500$ neurons was f. Due to the reduced firing rate between bursts dynamic synapses were able to partly recover and strongly respond at the bursts onset. The responses of the static synapses followed the unaltered mean firing rate f and thus could not discriminate the correlated bursts during the tone stimulus from the activity before the stimulus. For this CD task, detection requires $V_{pre-stim} < V_{th} < V_{stim}$, where $V_{pre-stim}$ (V_{stim}) represents the membrane potential during the pre-stimulus (stimulus) period. If one studies the detection for dynamic synapses as a function of the background frequency f_0 for constant, high, burst frequency f_1 one finds that $V_{pre-stim}$ increases and saturates with f and thus with the background frequency f_0 while V_{stim} decreases with increasing background frequency[8]. Since these two curves approach each other the area of good detection is again

[8] The membrane potential during the pre-stimulus period is $V_{pre-stim} \propto f\,w(f)$, where f equals the mean frequency during the stimulus period, i.e. $f = \frac{(N-M)}{N} f_0 + \frac{M}{N} f_1$ and $w(f)$ as given by equation (5.5). At the beginning of each burst, the membrane potential receives contributions from (a) a new bursting subpopulation, (b) other inputs that were previously bursting and (c) the remaining inputs, that is, $V_{stim} \propto \frac{M}{N} f_1 w(f_0) + \frac{M}{N} f_0 w(f_1) + \frac{(N-2M)}{N} f_0 w(f_0)$. This function is a decreasing function of f_0 when $1 + (f_1 - f_0)\tau_{rec} U_{SE} > \frac{N}{M}$, which is the case for the specific example considered in [20].

bell shaped and for the optimally chosen threshold value the detection is possible within the relatively large range of background frequency.

For the idealized case of coincident spike trains we have presented analytical results that show good agreement with numerical results. With this type of CD it is possible to derive analytical expressions that relate all relevant parameters and we have found how CD ability depends on other important parameters such as the number of coincident afferents (M) or the recovery time constant (τ_{rec}). We have not analysed how the CD is affected by the membrane time constant because this is already well explored in [17, 19] and it is expected to find better CD properties with smaller τ_m. The effects of temporal jitter are not thoroughly explored but it is worth mentioning that the jitter reduces the amount of synchrony decreasing the amplitude of the signal [19] and thus reduces the range of optimal thresholds for good detection.

We have not considered inhibitory inputs in this study, mainly because the dynamics of inhibitory synapses is less well established. It is expected that adding static inhibitory input will effectively reduce the threshold linearly with frequency. Therefore, in the presence of inhibition the CD with dynamic synapses is also expected to be superior.

It is known that in addition to depression, synapses also display short-term facilitation. The functional role of facilitation is less clear than for depression, since it has been demonstrated that pair pulsed stimulation, in addition to inducing LTP, will tend to reduce facilitation in favour of depression (synaptic redistribution) [5]. If it is true that LTP is a form of Hebbian learning and has therefore behaviour relevance for the animal, one should conclude that synaptic facilitation is of less functional relevance than depression. Nevertheless, the effects of facilitation on CD should be investigated.

Acknowledgments

Dr J J Torres acknowledges support from the 'Ministerio de Ciencia y Tecnologia' and FEDER ('Ramon y Cajal' contract and project no BFM2001-2841) and the Dutch Foundation for Neural Networks (SNN).

Appendix. Analytical results

Here we derive the analytical expressions that have been used to analytically compute equation (3.1). The total input current consists of a signal part and a noise part. We first treat the noise part and compute the number of the 'false-hits' (N_{falses}) considering only the mean level of the synaptic current. Then we compare this number with the corresponding value found by a more general noise treatment, i.e. by a hazard-function approximation [22]. We conclude that this approximation does not greatly change the effective level of the 'false-hits'. Furthermore we estimate the signal contribution and compute the number of 'failures' as well as the CD error (3.1).

4.1. Noise contribution

The noise part of the current consists of a large $(N - M)$ number of independent contributions, each one corresponding to a single synapse, that is $I = \sum_{i=1}^{N-M} I_i$. If a single spike arrives at the synapse i at time t^*, then for $t = t^* + \tau$ ($\tau > 0$) the current produced by this spike is given by

$$I_i(\tau; t^*) = I_{peak} \exp(-\tau/\tau_{in}); \tag{5.1}$$

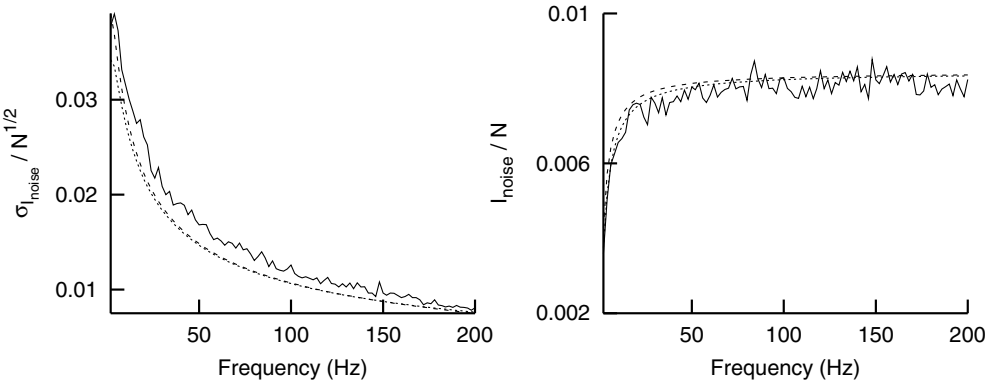

Figure A.1. Properties of the synaptic current with depressing synapses. Left: comparison between numerical current fluctuations computed for 200 depressing synapses (solid curve) and theoretical formula provided in equation (5.8) (dashed curve) and (5.6) (dotted curve). Right: mean synaptic current theoretically computed with formulae (5.7) (dashed curve) and (5.5) (dotted curve) compared with the numerical mean synaptic current for 200 depressing synapses (solid curve).

(cf equations (2.1)–(2.3)). Here, the amplitude I_{peak} represents the averaged stationary EPSC amplitude computed for a regular spike train which we assume also valid for the irregular case [1]

$$I_{peak} = A_{SE} \frac{U_{SE}(1 - \mathrm{e}^{-1/f\tau_{rec}})}{1 - (1 - U_{SE})\mathrm{e}^{-1/f\tau_{rec}}}. \tag{5.2}$$

We can compute the mean noise contribution of the current and the current fluctuations using the standard expressions

$$I_{noise} \equiv \langle I \rangle, \tag{5.3}$$

$$\sigma^2_{I_{noise}} \equiv \langle I^2 \rangle - \langle I \rangle^2. \tag{5.4}$$

From these definitions, using the central limit theorem and assuming $\tau_{in} \ll \tau_{rec}$ we obtain[9]

$$I_{noise} = (N - M) A_{SE} f \tau_{in} U_{SE} \frac{1 - \mathrm{e}^{-1/f\tau_{rec}}}{1 - (1 - U_{SE})\mathrm{e}^{-1/f\tau_{rec}}}, \tag{5.7}$$

and

$$\sigma^2_{I_{noise}} = (N - M) A^2_{se} \frac{\tau_{in} f (1 - \mathrm{e}^{-2/f\tau_{in}})}{2} \left(\frac{U_{se}(1 - \mathrm{e}^{-1/f\tau_{rec}})}{1 - (1 - U_{se})\mathrm{e}^{-1/f\tau_{rec}}} \right)^2 + \mathcal{O}(\tau^2_{in} f^2). \tag{5.8}$$

Figure A.1 shows a comparison between the numerical current-fluctuations and mean current for 200 dynamic synapses, and the corresponding analytical expressions (5.7) and (5.8) (dashed curve) as well as the analytical expressions (5.5) and (5.6) (dotted curve).

[9] Analogous expressions can be derived directly from equations (2.1)–(2.3) using different reasoning. One can obtain

$$I_{noise} = (N - M) A_{SE} \frac{f \tau_{in} U_{SE}}{1 + f \tau_{rec} U_{SE}} \equiv (N - M) f \tau_{in} w(f), \tag{5.5}$$

$$\sigma^2_{noise} = (N - M) \frac{f \tau_{in}}{2} \left(\frac{A_{SE} U_{SE}}{1 + f \tau_{rec} U_{SE}} \right)^2 = (N - M) \frac{f \tau_{in}}{2} w^2(f), \tag{5.6}$$

(for equation (5.5) see also [1]), where $w(f) = \frac{A_{SE} U_{SE}}{1 + f \tau_{rec} U_{SE}}$ can be interpreted as the stationary synaptic strength at frequency f. Assuming $f\tau_{rec} \gg 1$ and $\tau_{in} \to 0$, equations (5.7) and (5.8) reduce to equations (5.5) and (5.6) (cf figure A.1).

If we neglect the current fluctuations ($\sigma_{I_{noise}} = 0$), the membrane potential in the absence of an absorbing threshold is given by $V_{noise} = R_{in} I_{noise}$. From this expression we can compute the number of the 'false-hits'. False firing occurs when $V_{noise} > V_{th}$ and the total number of 'false-hits' in a period of time T is approximately given by $N_{falses} \approx T/(\tau_{ref} - \tau_m \ln(1 - V_{th}/V_{noise}))$ [15]. Then, we can relate N_{falses} with the number of the coincidence-input-events (N_{inputs}) using the fact that $T = N_{inputs}/f$. Thus, we obtain

$$N_{falses} = \frac{\theta(V_{noise} - V_{th}) N_{inputs}}{f[\tau_{ref} - \tau_m \ln(1 - V_{th}/V_{noise})]}, \tag{5.9}$$

where $\theta(x)$ is the Heaviside function. For $V_{noise} < V_{th}$ we have $N_{falses} = 0$.

In the presence of fluctuations, the expression (5.9) is not valid anymore and the number of 'false-hits' can be found in the following way. First, we have to rewrite the IF equation (2.4) by introducing a fluctuating term, that is,

$$\tau_m \, \mathrm{d}V(t)/\mathrm{d}t = -V(t) + \mathcal{I}(t) + \sigma_{\mathcal{I}} \sqrt{\tau_m} \xi(t), \tag{5.10}$$

where $\mathcal{I}(t) = R_{in} I_{noise}$, $\sigma_{\mathcal{I}}^2 = R_{in}^2 \sigma_{I_{noise}}^2$ and $\xi(t)$ is a Gaussian white noise with autocorrelation $\langle \xi(t)\xi(t') \rangle = \delta(t - t')$ (see [23]). For simplicity, let us first consider $\tau_{ref} = 0$ ms. In the presence of an absorbing threshold V_{th} the probability $\rho(\tau; t^*)$ of a spike occurring at time $t = t^* + \tau$, given the last spike at t^* defines a conditional inter-spike-interval (ISI) distribution. As suggested in [22] this distribution can be given by

$$\rho(\tau; t^*) = h(\tau; t^*) \exp\left[- \int_0^\tau h(s; t^*) \, \mathrm{d}s \right], \tag{5.11}$$

where $h(\tau; t^*)$ (a so-called *hazard function*) describes the risk of escape of the membrane potential across the threshold value. For the hazard function we use the Arrhenius ansatz [22] which depends only on the momentary distance between the noise-free membrane potential V_0 and the threshold V_{th} scaled by the noise amplitude, that is

$$h_{Arr}(\tau; t^*) = \Omega \exp\left\{ - \frac{(V_{th} - V_0(\tau; t^*))^2}{{\sigma_{\mathcal{I}}}^2} \right\} \tag{5.12}$$

where Ω represents a free parameter of the Arrhenius ansatz. To compute the ISI (equation (5.11)) we need to compute

$$\int_0^\tau h_{Arr}(s; t^*) \, \mathrm{d}s = \Omega \int_0^\tau \exp\left\{ - \frac{(V_{th} - V_0(s; t^*))^2}{{\sigma_{\mathcal{I}}}^2} \right\} \mathrm{d}s, \tag{5.13}$$

where $V_0(\tau; t^*) = V_{noise}[1 - \mathrm{e}^{-\tau/\tau_m}]$ is found by integration of the IF equation in the absence of an absorbing threshold [22].

The expression on the right-hand side of equation (5.11) is intractable and must be solved numerically. Then, we can compute the average time interval between two consecutive spikes by computing the average

$$\langle \tau \rangle = \frac{\int_0^\infty \tau \rho(\tau; t^*) \, \mathrm{d}\tau}{\int_0^\infty \rho(\tau; t^*) \, \mathrm{d}\tau}, \tag{5.14}$$

whose inverse gives the output frequency of the postsynaptic neuron, that is $f_{out} = 1/\langle \tau \rangle$. In figure A.2 we compare f_{out} theoretically computed with the Arrhenius ansatz (where the free parameter Ω has been chosen such to fit the numerical data, that is, $\Omega = 0.2$) and the numerical result for two different inputs frequencies showing a good fit of the escape noise ansatz approximation with the numerical data. The approximation fails near the critical V_{th} for nonzero output frequency.

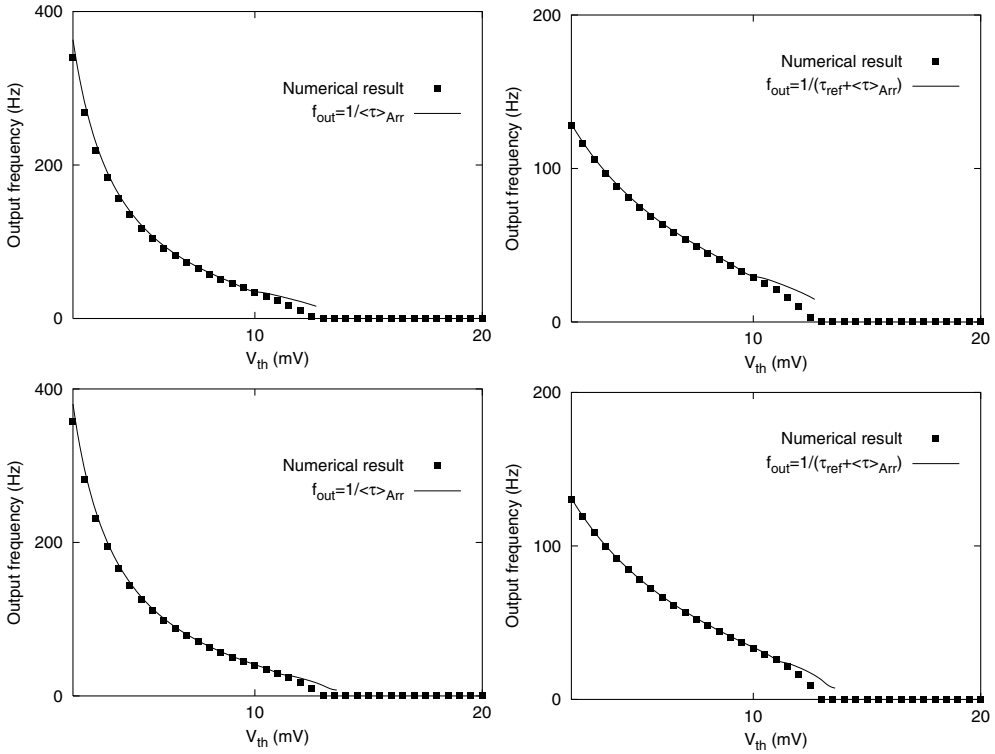

Figure A.2. Left: output frequency of the postsynaptic neuron receiving Poissonian spike trains from 800 afferents at input frequency $f = 30$ Hz (top) and $f = 80$ Hz (bottom) for $\tau_{ref} = 0$. Right: the same results for non-zero refractory period $\tau_{ref} = 5$ ms.

In the low-threshold region $N_{hits} \ll N_{falses}$, thus the number of the 'false-hits' is approximately given by

$$N_{falses} \approx T f_{out} = \frac{T}{\langle\tau\rangle}. \tag{5.15}$$

If we assume that in this region the number of failures is almost zero[10], the CD error (equation (3.1)) is given by

$$\text{Error} \approx \frac{N_{falses}}{N_{inputs}} = \frac{f_{out}}{f}. \tag{5.16}$$

Figure A.3 represents the curve $f_{out}/f = 1$ numerically computed for the non-zero refractory period of 5 ms (solid curve), the corresponding plot computed within the Arrhenius ansatz approximation (dashed curve) (note that for the non-zero refractory period $f_{out} = \frac{1}{\tau_{ref}+\langle\tau\rangle}$) and the same plot computed using equation (5.9) (dotted curve). The deviation of the Arrhenius ansatz approximation from the numerical result for low f is due to the fact that the Arrhenius ansatz approximation fails near the critical point, that is the point at which f_{out} becomes zero (cf figure A.2 (right)). The figure shows that above 30 Hz the analytical contour plot found by the Arrhenius ansatz approximation gives almost the same results as the analytical plot found with the analysis considering only the mean noise current. Therefore, we conclude

[10] This assumption is supported by numerical data.

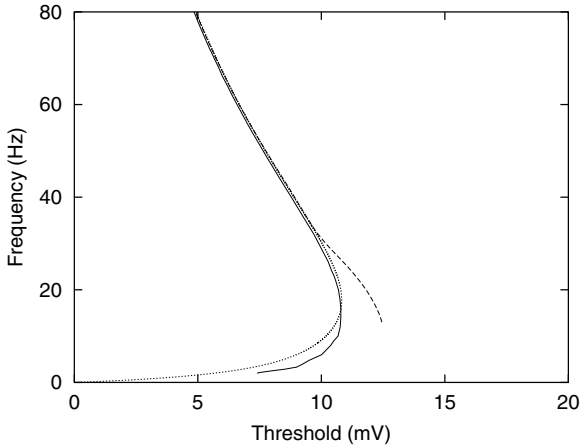

Figure A.3. The plot that corresponds to $f_{out} = f$. The solid curve represents the numerical results for the neuron receiving input from $N - M = 800$ afferents, the dotted curve denotes the analytical line found using equation (5.9) and the dashed curve corresponds to analytical results found using the Arrhenius ansatz approximation.

that the voltage level given by $V_{noise} = R_{in} I_{noise}$ is suitable to be used in equation (5.9) to compute the actual number of the 'false-hits'. For this reason we will also ignore fluctuations to compute the number of the 'failures' in further calculations.

Signal contribution

To analyse the signal contribution (arising from M coincident spikes) we first have to estimate the voltage level V_{signal}. Suppose, that the membrane potential at $t = t^*$ when M coincident spikes arrive is given by $V(0; t^*)$. Then, the membrane potential for $t = t^* + \tau$ ($\tau > 0$) can be computed by integration of the IF equation, that is

$$V(\tau; t^*) = \mathrm{e}^{-\tau/\tau_m}\left(V(0; t^*) + \frac{R_{in} M I_{peak}}{\tau_m \alpha}[\mathrm{e}^{\alpha\tau} - 1]\right), \tag{5.17}$$

where $\alpha = \frac{\tau_{in} - \tau_m}{\tau_{in}\tau_m}$. If the next signal ($M$ coincident spikes) occurs at $t = t'$, we can obtain the following recurrence relation:

$$V(0; t') = \mathrm{e}^{-\Delta t/\tau_m}\left(V(0; t^*) + \frac{R_{in} M I_{peak}}{\tau_m \alpha}[\mathrm{e}^{\alpha\Delta t} - 1]\right), \tag{5.18}$$

where $\Delta t = t' - t^*$. From this relation we can compute the stationary value for the membrane potential at the exact time of signal arrival, that is

$$V_{st} = \mathrm{e}^{-\Delta t/\tau_m}\frac{R_{in} M I_{peak}}{\tau_m \alpha}\frac{(\mathrm{e}^{\alpha\Delta t} - 1)}{(1 - \mathrm{e}^{-\Delta t/\tau_m})}; \tag{5.19}$$

(see also [18]). Furthermore, we need to compute the maximum of the membrane potential between consecutive EPSC signal events that we define as V_{signal}. This can be easily computed from equation (5.17), with $V(0; t^*)$ replaced by V_{st}:

$$V_{signal} = \left[\frac{\tau_m(1 - \mathrm{e}^{-1/f\tau_m})}{\tau_{in}(1 - \mathrm{e}^{-1/f\tau_{in}})}\right]^{\frac{\tau_m}{\tau_{in} - \tau_m}} R_{in} M I_{peak}, \tag{5.20}$$

where $f = 1/\Delta t$. The number of failures $N_{failures}$ counts the number of times the voltage produced by 'signal' plus 'noise' does not reach the threshold value and can be obtained from

$$N_{failures} = N_{inputs} - N_{hits}, \tag{5.21}$$

where N_{inputs} and N_{hits} count the number of the 'coincident-input-events' and the number of the 'hits', respectively. If the level of the signal V_{signal} is higher than V_{th}, every 'coincident-input-event' produces a 'hit' and the number of failures is zero. Otherwise, when $V_{signal} < V_{th}$ we have

$$N_{failures} = N_{inputs}\left[1 - \frac{\theta(V_{noise} + V_{signal} - V_{th})}{f(\tau_{ref} + \tau_1)}\right], \tag{5.22}$$

where $\theta(x)$ is the Heaviside function whereas τ_1 represents the rising time of the membrane potential (after the absolute refractory period) and can be found from $V_0(\tau_1; t^* + \tau_{ref}) + V_{signal} = V_{th}$. Finally, from last expressions we obtain

$$N_{failures} = N_{inputs}\left[1 - \frac{\theta(V_{noise} + V_{signal} - V_{th})}{f\left[\tau_{ref} - \tau_m \ln\left(1 - \frac{V_{th} - V_{signal}}{V_{noise}}\right)\right]}\right], \tag{5.23}$$

where for $V_{noise} + V_{signal} < V_{th}$ we have $N_{failures} = N_{inputs}$. From equations (5.23) and (5.9) we analytically compute the CD error (3.1) (cf figures 2, 3).

References

[1] Tsodyks M and Markram H 1997 *Proc. Natl Acad. Sci. USA* **94** 719
[2] Abbott L F, Varela J A, Sen K and Nelson S B 1997 *Science* **275** 220
[3] Abeles M 1982 *Isr. J. Med. Sci.* **18** 83
[4] Abeles M 1982 *Local Cortical Circuits* (Berlin: Springer)
[5] Markram H and Tsodyks M 1996 *Nature* **382** 807
[6] Markram H, Wang Y and Tsodyks M 1998 *Proc. Natl Acad. Sci. USA* **95** 5323
[7] Dobrunz L and Stevens C 1997 *Neuron* **18** 995
[8] Stevens C and Wang Y 1995 *Neuron* **14** 795
[9] Decharms R C and Merzenich M M 1996 *Nature* **381** 610
[10] Wehr M and Laurent G 1996 *Nature* **384** 162
[11] Stopfer M, Bhagavan S, Smith B H and Laurent G 1997 *Nature* **390** 70
[12] Steinmetz P N, Roy A, Fitzgerald P J, Hsiao S S, Johnson K O and Niebur E 2000 *Nature* **404** 187
[13] Hodgkin A and Huxley A 1952 *J. Physiol.* **117** 500
[14] Tuckwell H 1988 *Introduction to Theoretical Neurobiology vol 1 and 2* (Cambridge: Cambridge University Press)
[15] Koch Ch 1999 *Biophysics of Computation: Information Processing in Single Neurons* (New York: Oxford University Press)
[16] Konig P, Engel A and Singer W 1996 *Trends Neurosci.* **19** 130
[17] Kempter R, Gerstner W, van Hemmen J L and Wagner H 1998 *Neural Comput.* **10** 1987
[18] Kistler W M and van Hemmen J L 1999 *Neural Comput.* **11** 1579
[19] Marsalek P 2000 *Biosystems* **58** 83
[20] Senn W, Segev I and Tsodyks M 1998 *Neural Comput.* **10** 815
[21] Salinas E and Sejnowski T J 2000 *J. Neurosci.* **20** 6193
[22] Plesser H E and Gerstner W 2000 *Neural Comput.* **12** 367
[23] Brunel N 2000 *J. Comput. Neurosci.* **8** 183